Resistance to Recrystallization in Al-1% Mn Alloys

Fernando Cerqueira Pimenta Jr.*, Antonio Celso F. Arruda, and Angelo Fernando Padilha**

(*Instituto de Pesquisas Tecnológicas do Estado de São Paulo S. A., São Paulo, **Faculdade de Engenharia Mecânica, Universidade de Campinas, Campinas, and Instituto de Pesquisas Energéticas e Nucleares, P. O. Box 11049, São Paulo, Brasil)

The microstructure of comercial grade Al-1% Mn alloy was studied after various heat, mechanical and thermal treatments with the aid of various complementary microstructural analysis techniques. Three phases, namely the matrix, the precipitates of $Al_6(Mn,Fe)$ and the precipitates of α-AlFeMnSi have been identified. The quantity, size, composition and structure of these phases have been studied. Subsequently, the influence of prior stabilizing heat treatment at 370 °C and partial solubilization at 630 °C on work hardening, recrystallization and recrystallized grain size have been studied. The treatment at 630 °C resulted in more pronounced work hardening, higher resistance to recrystallization and smaller recrystallized grain size than the treatment at 370 °C. The study has indicated that the treatment at 630 °C together with an adequate degree of deformation produces microstructures higly resistant to recrystallization.

Rekristallisationswiderstand von Al-1%-Mn-Legierungen

Es wurden die bei zahlreichen thermischen und thermomechanischen Behandlungen von Al-1% Mn technischer Zusammensetzung auftretenden Gefügeänderungen mit verschiedenen sich ergänzenden metallkundlichen Methoden untersucht. Drei Phasen – die Matrix und die Ausscheidungen $Al_6(Mn, Fe)$ und α-AlFeMnSi – wurden nachgewiesen und deren Menge, Größe, Zusammensetzung und Struktur bestimmt. Danach wurde der Einfluß der vorausgehenden Stabilisierungsauslagerung bei 370 °C und der partiellen Lösungsglühung bei 630 °C auf die Verfestigung, auf die Rekristallisation und auf die rekristallisierte Korngröße untersucht. Die Glühung bei 630 °C verursachte stärkere Verfestigung, sowie stärkeren Rekristallisationswiderstand und kleinere rekristallisierte Korngröße, als die Auslagerung bei 370 °C. Diese Untersuchung zeigt, daß die Glühung bei 630 °C verknüpft mit einem passenden Verformungsgrad Gefüge mit sehr starkem Rekristallisationswiderstand erzeugt.

1 Introduction

From the point of view of mechanical strength there is still a large gap between the non-heat-treatable wrought aluminium alloys and the precipitation hardenable aluminium alloys.

In the annealed state the 3000 series (Al, Mn, Fe, Si) aluminium alloys, when compared to the commercially pure aluminium (Al, Fe, Si), exhibit higher mechanical strength, slightly lower ductility and comparable corrosion resistance. The alloy 3003 is not precipitation hardenable. Also, due to the low solubilities of Mn, Fe and Si in these alloys, solid solution hardening does not exercise any significant influence. The precipitate particles present in the microstructure are in general large primary incoherent precipitates, not prone to shearing and cause dispersion hardening to a small extent. Work hardening is an alternative, especially in alloys that are disperison hardenable, since they exhibit higher work hardening rates. In this respect, procedures that inhibit recrystallization, take on greater importance. This fact justifies the increased interest in the study of recrystallization and related phenomena in these alloys[1) to 10)].

The alloy 3003 also does not reveal any significant grain growth after recrystallization[11)], since the precipitates act as barriers for the migration of grain boundaries. However, further information about the recrystallization kinetics, especially about the variables that influence recrystallized grain size, are important for their control. The main aim of this investigation has been to explore some of the procedures available for inhibiting recrystallization and or refinement of the recrystallized grain size in alloy 3003.

2 Experimental Procedure

The alloy used was fabricated commercially by semicontinuous casting of plate type ingots 250 mm thick. The ingots were then homogenized between 600 and 635 °C during about 8 h and hot rolled to a thickness of 6 mm. The chemical composition of the heat studied was, by weight: 0.90 % Mn; 0.65 % Fe; 0.19 % Si; 0.14 % Cu; 0.014 % Ti and other elements in concentrations less than 0.01 %. All the heat treatments, those preceeding and succeeding cold work were carried out in sodium nitrate baths. All the specimens were rolled at room temperature in a duo-reversible rolling mill with rolls 130 mm in diameter. The actual deformation (E) was calculated using the formula $E = \ln (e_i/e_f)$ where e_i and e_f are the initial and final thickness, respectively.

The microstructure of the alloy in the different stages was studied with the aid of a number of complementary techniques. The morphology, quantity, size and distribution of the various phases present were studied by optical microscopy. The specimens for optical microscopy and microhardness testing were electrolytically polished in a solution containing 700 ml ethyl alcohol, 120 ml distilled water, 100 ml butyl glycol and 68 ml perchloric acid. The polishing was carried out at 14 V for 20 s. Unetched specimens had been studied under conventional illumination. In order to closely observe recrystallization in the specimens, the polished specimens were anodized and observed under polarized light. The electrolyte used for anodization was that proposed by Barker[12)] and consisted of 9 ml fluoboric acid in 400 ml of distilled water. The spec-

imens were anodized for 60 s at 20 V. This technique allows clear identification of the recrystallized and the non-recrystallized regions. The different phases present were analyzed with the aid of a microprobe analyzer.

The lattice parameter was determined by X-ray diffractometry of polished surfaces. The precipitates to be analyzed by X-ray diffraction had to be isolated from the matrix. Two different methods were tried out to dissolve the matrix: one electrochemical, using the solution mentioned above for polishing and the other chemical, suggested by Sperry[13]), where a solution of iodine in methanol was used. After dissolving the matrix, the precipitates were separated by filtering the solution through a PTFE membrane with a pore size of 0.2 μm, washed, dried and analyzed in a Debye-Scherrer camera. Cu-Kα radiation was used in the two cases. The dislocation substructure was observed in a transmission electron microscope. The thin foils for TEM were obtained by electrolytic polishing, in the same solution used for the preparation of specimens for optical microscopy. The voltage used in this case was, however, 50 volts. In all the specimens, at least 7 Vickers microhardness identations were carried out under a load of 0.1 kg.

3 Results

3.1 Characterization of the Phases Present

3.1.1. As-Received Material

Polarized light optical microscopy of anodized specimens and microhardness measurement helped conclude that the hot rolled material was not completely recrystallized. Figure 1 reveals some of the aspects observed by TEM. The grains can be seen to be divided into subgrains with diameters in the range of 1 to 6 μm. The subgrains contain dislocation networks. Besides the dislocation substructure, the presence of two classes of precipitates that vary in size can also be observed: large numbers of very fine precipitates < 0.3 μm and large precipitates with sizes comparable to those of the subgrains. The large precipitates are most probably primary precipitates whereas the fine precipitates could have formed during thermomechanical processing of the material. Details of the larger precipitates can be seen in Fig. 2. A number of dislocations can be seen within the larger precipitate indicating that these precipitates can accomodate a degree of deformation. Electron diffraction of these precipitates revealed that they had an orthorhombic structure.

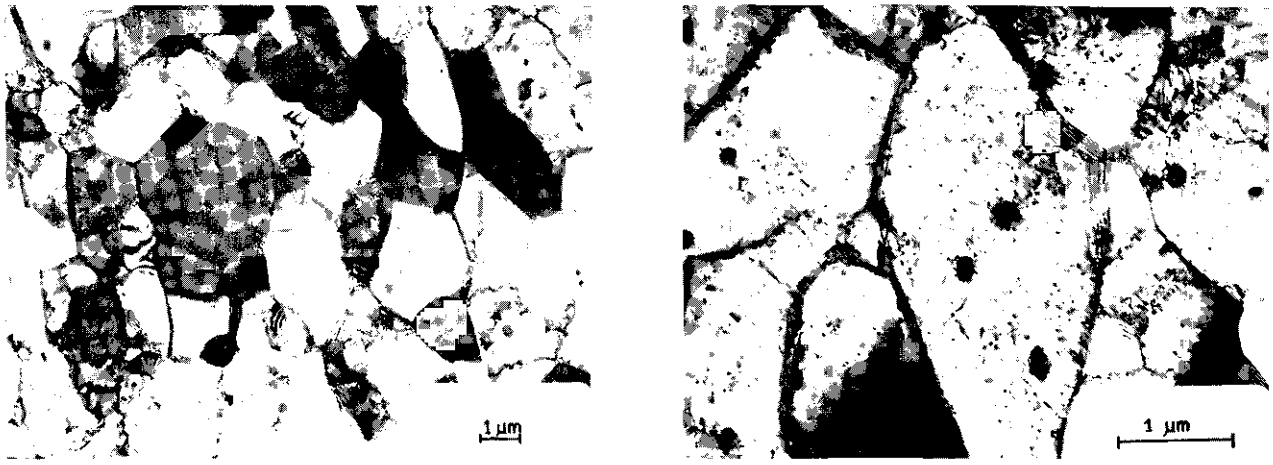

Fig. 1. Transmission electron micrographs of the as received material revealing subgrains and precipitate particles.

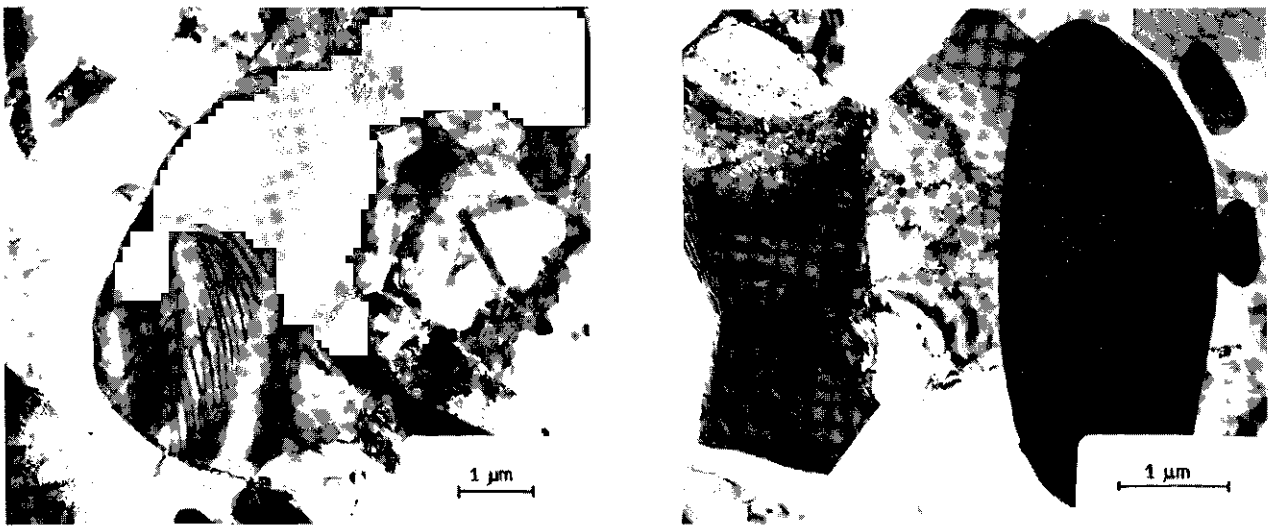

Fig. 2. Transmission electron micrographs showing larger particles of precipitates.

3.1.2. Thermal Pretreatments

Prior to cold working the specimens were divided into two group based on the specific heat treatments given. Group A specimens were stabilized at 370 °C for 10 h and air cooled. Group B specimens had been partially solubilized at 630 °C for 2 h followed by quenching in water.

The quantity of the phases present were determined by quantitative metallography, carried out with the aid of an optical microscope. Particles smaller than the resolving power of the microscope, about 0.5 μm, were not considered. The results are shown in Table 1. It can be seen that initial heat treatments altered only slightly the volume fraction of precipitates. The size of the phases were also studied by optical microscopy. Specimens belonging to both groups, A and B, revealed grains totally recrystallized with average diameters 83.0 $\pm$ 11.3 and 81.9 $\pm$ 13.3 μm, respectively. Average precipitate size measurements were also carried out. Optical microscopic measurements gave the impression that only one type of particle was present, gray in color and rod like in morphology. The larger and the smaller dimensions of each of the precipitates were measured, and the average size determined as the arithmetic average of the two measurements. Only precipitates with smaller dimension greater that 0.5 μm were considered and nearly 800 precipitates in each of the two groups of specimens measured. Figure 3 shows the size distribution of the two groups. The results reveal that both the matrix grain size and the precipitates size are almost identical for the two groups.

The partition of the alloying elements in the phases were studied by wavelength analysis in an electron probe analyzer. It was found that: a) all the Mn, Fe and Si were mainly concentrated in the particles; b) all the particles contained Mn and Fe; and c) not all particles contained Si. These results are in accordance with those reported in literature[3)5)8)], where it is stated that in this alloy two types of precipitates are to be found with distinct compositions: one that dissolves Si, α-AlFeMnSi and other that does not dissolve Si, $Al_6(Mn,Fe)$.

The crystal structures of the phases were studied by X-ray diffraction. The lattice parameter of the matrix is shown in Table 2 and compared with that of pure Al. The coincidence of the lattice parameter values for pure Al and that for the alloy confirms the previously mentioned low solubility of Mn, Fe and Si in this alloy. The low volumetric

Table 1. Volumetric fraction of precipitates for different treatment.

as received	0.049 $\pm$ 0.012
Group A	0.039 $\pm$ 0.011
Group B	0.035 $\pm$ 0.014

Table 2. Lattice parameters of the specimens.

ao (Å)	reference	alloy
4.05	this work	3003
4.0494	14)	pure Al
4.0497	15)	pure Al

AVERAGE SIZE (μm)	DISTRIBUTION(%)
Dm < 2	40.71
2 < Dm < 3	41.30
3 < Dm < 4	12.31
4 < Dm < 5	4.02
Dm ≥ 5	1.66

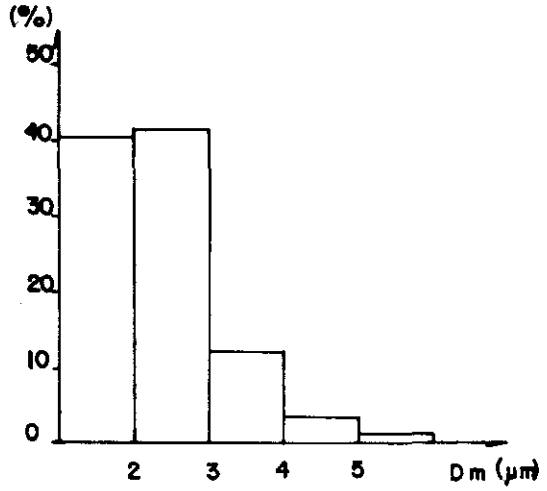

Fig. 3a. Specimen stabilized at 370 °C for 10 h and air cooled (group A).

AVERAGE SIZE (μm)	DISTRIBUTION(%)
Dm < 2	31.62
2 < Dm < 3	33.29
3 < Dm < 4	14.78
4 < Dm < 5	10.53
5 < Dm < 6	3.98
6 < Dm < 7	3.59
Dm > 7	2.21

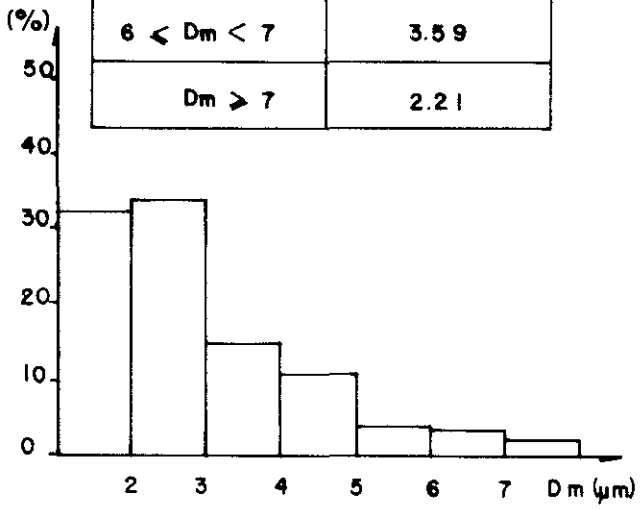

Fig. 3b. Specimen partially solubilized at 630 °C for 2 h and water quenched (group B).

Fig. 3a and b. Distribution of average size of precipitates.

fraction of the precipitates precluded their study by diffractometry of polished surfaces. This necessitated extraction of the precipitates for subsequent study by X-ray diffraction in a Debye-Scherrer camera. An electrochemical method had to be used to separate the precipitates from the matrix, since the solution of iodine in methanol was found to attack the precipitates. The $Al_6(Mn,Fe)$ phase data coincided well with those from the JCPDS card and was found to be orthorhombic Al_6Mn[16]. On the other hand, the lines of the α-AlFeMnSi phase coincided only reasonably well with the lines from the JCPDS card for the hexagonal α-AlFeSi[17]. Nevertheless it can be stated that there is agreement among various authors[18][19] about the cubic structure of the quaternary phase, α-AlFeMnSi. It should however be mentioned that it was not possible to correlate the two types of precipitates with the two size classes mentioned earlier.

3.2 The Cold Worked State

Figure 4 shows the curves of hardness versus degree of cold work for the two groups of specimens. It can be seen that group B specimens systematically showed higher hardness. TEM observations also showed considerable differences in the cold worked substructure of the two groups of specimens. For a certain degree of cold work, specimens that had previously been solubilized (group B) showed a higher dislocation density, with their deformation cells poorly defined and contained more dislocations in the cell interiors than the specimens that had previously been stabilized (group A). Furthermore, group B specimens showed a number of dislocation loops, that had most probably formed due to coalescence of vacancies retained by the high cooling rates.

3.3 Annealing of the Cold Worked Specimens

Work hardened specimens belonging to the two groups were annealed for 1 h at 370 °C. Figure 5 shows the curves of hardness versus degree of cold work, after this annealing treatment, for both groups of specimens. It can be seen that group B specimens, although in the cold worked state showed higher hardness, higher dislocation density and thereby a higher driving force for recrystallization, did not recrystallize at this annealing temperature. In order to evaluate the extent of the resistance to recrystallization, the specimen with the highest degree of cold work ($E = 0.7$) was further annealed for 10 h (shown with * in Fig. 5) and though soft due to recovery, did not show any new recrystallized grain. Specimens of this group were studied by TEM and as can be seen from Fig. 6, the dislocation rearrangement, the subgrain migration and thereby the nucleation of new recrystallized grains were inhibited by the reprecipitation of fine particles. On the other hand, group A specimens showed increasing fractions of recrystallized areas with increasing cold work. Specimens of this group deformed to 0.4 and 0.7 were annealed for different durations at 370 °C and their recrystallization kinetics studied. The specimen cold worked to 0.4, after annealing for only 2 min, showed the recrystallized fraction to be around 10 %, and in that annealed for 36 h the recrystallized fraction was found to be only around 13 %. These non-recrystallized regions however, showed a considerable degree of softening due to recovery processes. Specimens deformed to 0.7 after annealing for 1 min showed the recrystallized fraction to be 91 % and that annealed for 3 h to be only 93 %. Generalizing, it can be said that specimens of this group did not recrystallize completely at this temperature and that the residual non-recrystallized volumetric fraction increased with decreasing degree of cold work. Specimens with higher degree of cold work (for example $E = 1.2$) and annealed at 370 °C or specimens cold worked to 0.4 and annealed at higher temperatures (for example 500 °C) were found to be completely recrystallized.

In order to evaluate better the resistance to recrystallization, cold worked specimens 0.3 and 0.7 of the two groups were annealed for 1 h at different temperatures in the range 240 to 530 °C. These results are shown in Fig. 7; and the exceptional resistance of group B specimens to recrystallization can be seen. For example, group B spec-

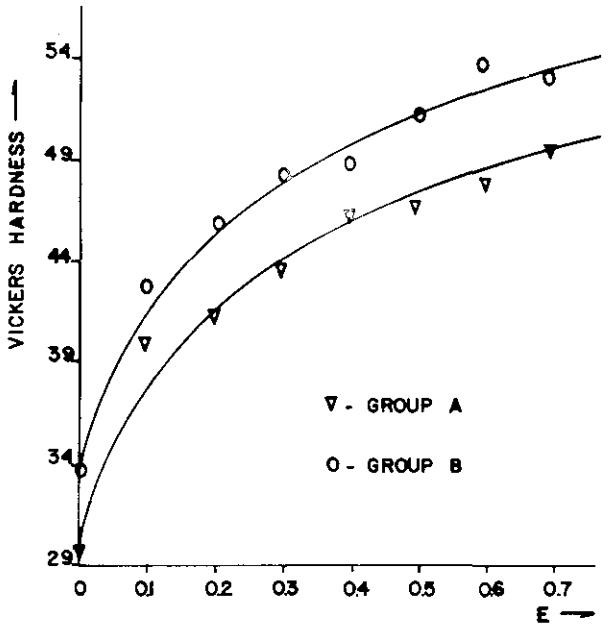

Fig. 4. Variation of Vickers microhardness with degree of deformation for the two groups of specimens.

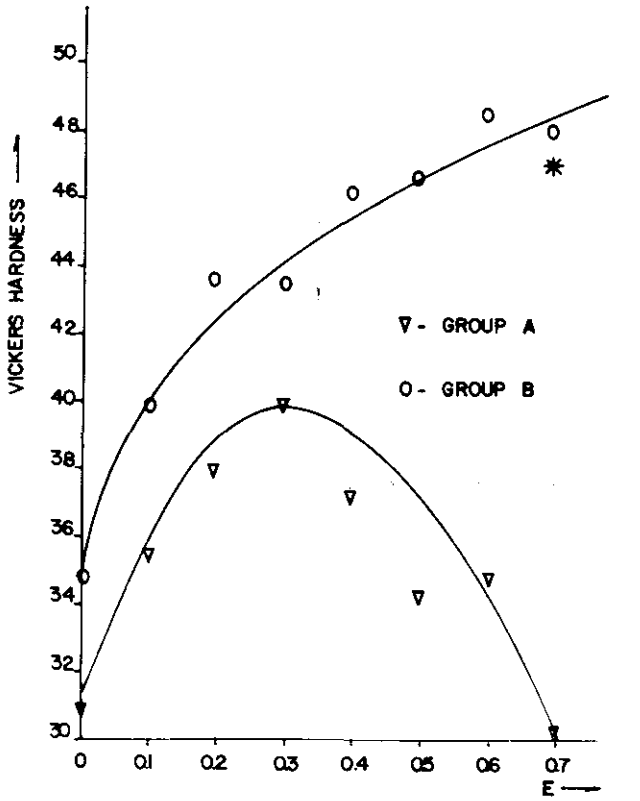

Fig. 5. Influence of annealing at 370 °C for 1 h on specimens of the two groups with different degree of deformation.

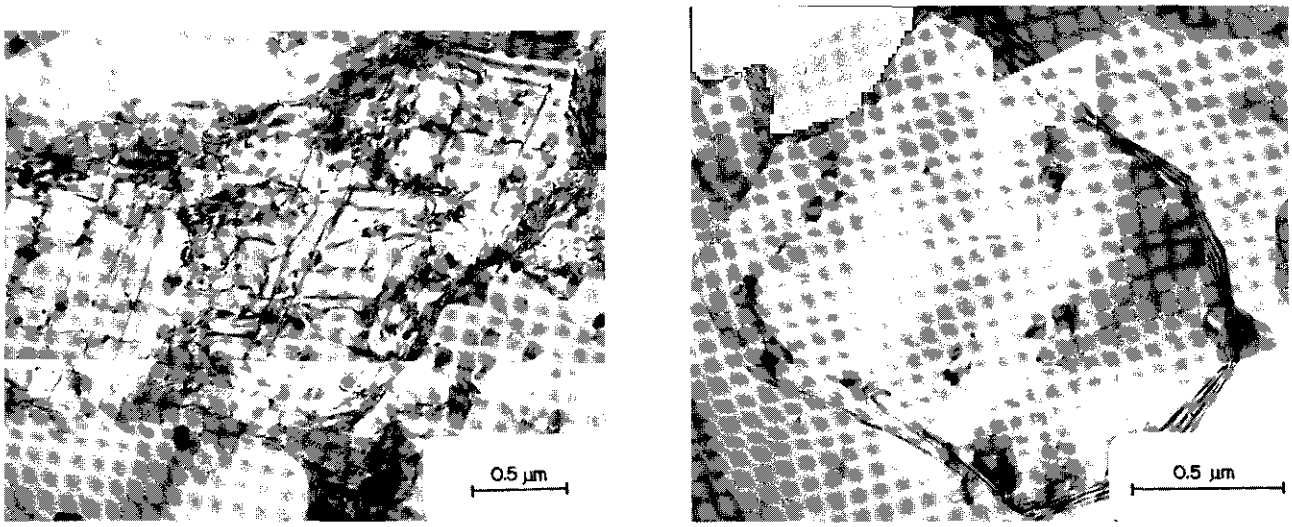

Fig. 6. Transmission electron micrographs of specimens solubilized at 630 °C for 2 h, cold worked with $E = 0.7$ and annealed at 370 °C for 11 h.

imens deformed to $E = 0.7$ exhibit a higher resistance to recrystallization than group A specimens deformed to only 0.3.

In order to evaluate the influence of pretreatments on the recrystallized grain size, specimens of two groups, deformed to 0.3 and 0.7, were completely recrystallized at 530 °C for 1 h and their grain sizes measured. It can been seen from Table 3 that group B specimens, which had shown higher degrees of work hardening and higher resistance to recrystallization when recrystallized, revealed grain sizes smaller than those of group A specimens.

Table 3. Mean diameter of the grains ($\bar{D}$) after annealing at 530 °C for 1 h in specimens of the two groups and for two degrees of predeformation E.

Group	E	$\bar{D}$ (µm)
A	0.7	43.6 ± 5.4
B	0.7	39.3 ± 6.7
A	0.3	94.4 ± 12.4
B	0.3	61.3 ± 2.9

4 Discussion

4.1 The Phases Present

One of the first papers on the phases present in alloy 3003 was by Sperry[13]), who identified four phases in the as-cast alloy; the matrix, precipitates of $Al_6(Mn,Fe)$, α-Al(Mn,Fe) and Si. Furrer and Hausch[5]) found with the aid of more advanced techniques the presence of only two precipitates in the as-cast alloy; $Al_6(Mn,Fe)$ about 85 % by volume and α-$Al_{12}(Fe,Mn)_3Si$ about 15 %. After homogenization at 620 °C for 16 h the quantitiy of $Al_6(Mn,Fe)$ decreased from 85 % to 35 % with a corresponding increase in the quantity of the α-phase. In a recent paper, Mathew and co-authors[19]) reported that after homogenization at 645 °C, the alloy revealed the presence of only the α-phase. In this paper, where hot rolled sheets have been used, different complementary techniques have shown the presence of two phases, namely α-Al(Fe,Mn)Si and $Al_6(Mn,Fe)$. X-ray diffraction analysis of the extracted residue revealed that the quantity of the α-phase in the residue was slightly higher. This analysis also indicated that after thermo-mechanical treatments of the alloy, the relative quantities of the phases were close to the equilibrium values and little change if any took place after subsequent heat treatments, even at temperatures as high as 630 °C. With respect to the crystalline structure, almost all the published literature mention the phase $Al_6(Mn,Fe)$ to be orthorhombic whereas doubts still exist about the structure of the α phase. Munson[18]) suggests that the ternary phase α-AlFeSi has a hexagonal structure and that the quaternary phase α-AlFeMSi, where M can be V, Cr, Mn, Cu, Mo or W has a bcc structure. Both, Furrer and Hausch as well as Mathew and co-authors indexed the alloy 3003 to be cubic. The X-ray diffraction results of this paper do not permit the affirmation that this phase is not hexagonal.

4.2. The Work Hardening Behaviour

Specimens of both groups showed a considerable degree of work hardening, a characteristic feature of alloys dispersion hardened by incoherent particles[20]). The differences observed between the two groups of specimens after deformation will be discussed on the basis of the relevant hardening mechanisms; namely grain boundary hardening, particle hardening, solid-solution hardening and quench hardening. Since the grain size of the matrix, the volumetric fraction and the particle size distribution in the two groups of specimens were almost identical, "a priori" the grain boundary hardening and the particle hardening mechanisms can be excluded as mechanisms responsible for the observed differences in the degree of work hardening between the groups. If the particle hardening mechnisms is considered to be responsible for the observed differences, specimens of group A, which showed slightly higher volumetric fraction for the same average size, should have revealed a higher degree of work hardening than the specimens of group B. On the other hand, solid-solution hardening and quench hardening exercise considerable influence both on work hardening and on the processes that occur during subsequent annealing of the work hardened material. Transmission electron microscopic observations suggest that quench hardening plays a more dominant influence on work hardening, while solute reprecipitation plays a greater role in recrystallization delays. This interpretation is in agreement with literature, which has shown that quenching has a considerable hardening effect[21]) and in-

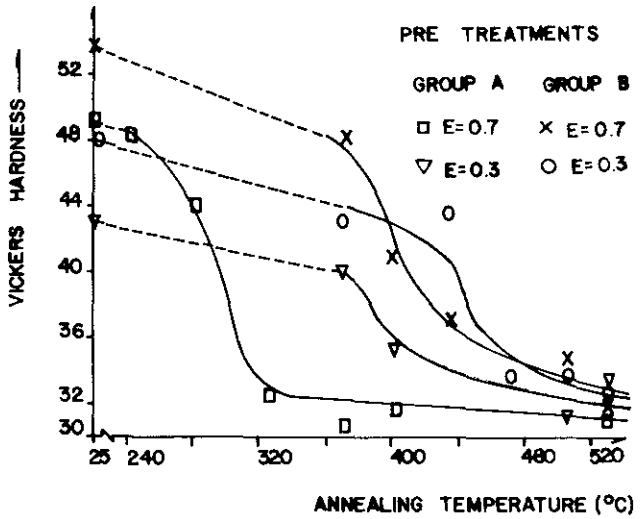

Fig. 7. Effect of 1 h isochronous annealing on specimens of the two groups for two degree of deformation.

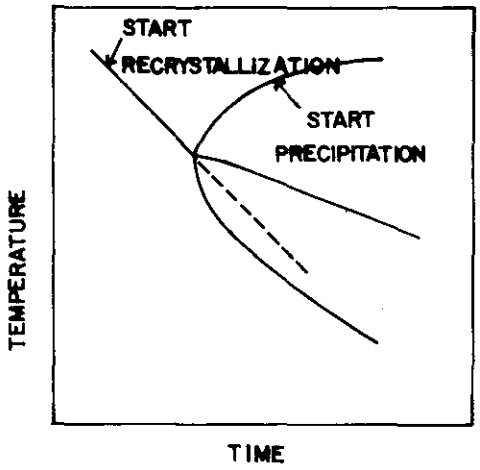

Fig. 8. TTT diagram illustrating interactions between precipitation and recrystallization[26]).

hibits the formation of deformation cells in Al[22]). Nevertheless, the dislocation loops, caused by quenching, do not have sufficient thermal stability[23]) to retard recrystallization, and its effect is only indirect. The effect of reprecipitation on recrystallization at temperatures below 630 °C will be discussed in the next section.

4.3 Recovery and Recrystallization

The interpretation of the results can be made easy if recrystallization can be defined as the migration of high angle boundaries under influence of driving and dragging forces. Stüwe[24]) evaluated a number of possible driving forces, such as energy stored from cold work, grain boundary energy, surface energy, magnetic energy and discontinuous precipitation, as well as dragging forces such as second phase particles, solute atoms and surface grooves that could have an influence on the boundaries during recrystallization. In this paper, only the three more important forces have been considered: stored energy from cold work, grain boundary energy as driving forces and second phase particles as the dragging force. For example, the fact that grain growth after recrystallization does not take place can be explained by a balance between the forces acting on the boundaries. Assuming a volumetric fraction of 4 % for particles with an average radius of 2 μm and grain boundary energy of 0.5 J/m^2, a retarding force of $3 \cdot 10^4$ N/m^2 is obtained using Zener's formula[25]). This force which inhibits the movement of the boundaries is more than twice the total grain boundary energy, $1.25 \cdot 10^4$ N/m^2, for a material with an average grain diameter of 80 μm, which is the driving force for grain growth. On the other hand, the energy stored due to deformation, considering only the dislocations, is of the order of 10^8 N/m^2, for a dislocation density of the order of 10^{12} cm/cm^3. Nevertheless, the resistance imposed by the precipitates may have only a minor influence on the recrystallization of alloys with dispersed precipitates when the grain boundary moves across obstacles under the action of a high driving force. High driving force situation occur, for example, during high degrees of deformation and at the initiation of recrystallization, when the release of substantial quantities of energy stored during deformation does not take place due to recovery of non-recrystallized regions. As long as the energy stored during deformation decreases, due either to reduction in degree of deformation or to the recovery of non-recrystallized regions during annealing, the resistance imposed by the precipitates plays an increasingly important part in recrystallization kinetics. At low levels of deformation, the number of recrystallization nuclei and the driving force for recrystallization are lower. Under these conditions, the high angle boundaries should migrate greater distances at low velocities – the velocity of migration of the boundaries is proportional to the driving force – requiring more time, during which extensive recovery of the non-recrystallized regions can take place, reducing the energy stored during deformation to the point that restrictions imposed by the precipitates obstructs the migration of the boundaries. This high degree of recovery explains the residual non recrystallized fraction which increase with decreasing degree of deformation in specimens of group A. Padilha and Falleiros[7]) found that in alloy 3003 at low levels of deformation there was a considerable decrease in the velocity of migration of boundaries with annealing time, due to recovery of non recrystallized regions. They also found that beyond a certain recrystallized volumetric fraction, which decreased with decreasing degree of deformation, the equation of Avrami no longer describes recrystallization kinetics.

In the specimens of group B there was the additional precipitation of particles during annealing, inhibiting the rearrangement of dislocations and the growth of the subgrains, shifting the formation of the recrystallization nuclei to longer times or higher temperatures, as illustrated schematically in Fig. 8. However, the reduction in migration velocity of the boundaries should be even more pronounced than the reduction in the velocity of nucleation to justify the smaller grain sizes obtained in the specimens of group B in comparison to those obtained in the corresponding specimens of group A.

Literature

1) E. NES and J. D. EMBURY, Z. Metallkde. **66** (1975) 589–593.
2) E. NES, Acta Metall. **24** (1976) 391–398.
3) P. L. MORRIS and B. J. DUGGAN, Metal Science **121** (1978) 1–7.
4) G. HAUSCH, P. FURRER and H. WARLIMONT, Z. Metallkde. **69** (1978) 174–180.
5) P. FURRER and G. HAUSCH, Metal Science **13** (1979) 155–162.
6) E. NES and S. SLEVALDEN, Aluminium **55** (1979) 319–324.

[7]) A. F. PADILHA and I. G. S. FALLEIROS, Metalurgia – ABM **35** (1979) 587–590.
[8]) D. J. LLOYD, Metal Science **16** (1982) 304–308.
[9]) C. DIALLO, Thése no. 485, École Polytechnique Fédérale de Lausanne, Lausanne (1983).
[10]) E. NES, N. RYUM and O. HUNDERI, Acta Metall. **33** (1985) 11–22.
[11]) P. A. BECK, M. L. HOLZWORTH and P. R. SPERRY, Trans. Met. Soc. AIME **180** (1949) 163–192.
[12]) L. J. BARKER, Trans. ASM **42** (1950) 347–356.
[13]) P. R. SPERRY, Trans. AIME – J. Metals **7** (1955) 145–151.
[14]) Powder diffraction file 4-0787 (Al) Joint Comittee on Powder Diffraction Standards.
[15]) B. D. CULLITY, Elements of X-ray Diffraction, 2nd edition, Addison Wesley Publ., New York (1978) 506.
[16]) Powder diffraction file 6-0665 (Al_6Mn), Joint Comittee on Powder Diffraction Standards.
[17]) Powder diffraction file 20–30 (α-AlFeSi), Joint Comittee on Powder Diffraction Standards.
[18]) D. MUNSON, J. Inst. Met. **95** (1967) 217–219.
[19]) E. V. MATHEW, J. R. RAMACHANDRAN, K. P. GUPTA and S. DAS, J. Mater. Sci. Letters **3** (1984) 605–610.
[20]) A. KELLY, R. B. NICHOLSON, Precipitation Hardening, 1st. edition, B. Chalmers (ed.), Progress in Materials Science. Volume 10, Pergamon Press, New York (1963) 313.
[21]) R. MADDIN and A. H. COTTRELL, Phil. Mag. **46** (1955) 735–744.
[22]) R. VANDERVOORT and J. WASHBURN, Phil. Mag. **5** (1960) 24–29.
[23]) P. W. SHIN and M. MESHII, J. Metals **15** (1963) 80–87.
[24]) H. P. STÜWE, in: Recrystallization of Metallic Materials, 2nd edition, F. Haessner (ed.), Dr.-Riederer-Verlag, Stuttgart (1978) 11–21.
[25]) C. S. SMITH, Trans. Met. Soc. AIME **175** (1948) 15–51.
[26]) E. HORNBOGEN, in: Recrystallization of Metallic Materials, 2nd edition, F. Haessner (ed.), Dr.-Riederer-Verlag, Stuttgart (1978) 159–194.

(Eingegangen am 3. Februar 1986)